PHYSICAL REVIEW D **93,** 065056 (2016)

Phase diagrams of the multitrace quartic matrix models of noncommutative Φ^4 theory

B. Ydri,* K. Ramda, and A. Rouag

Department of Physics, Faculty of Sciences, Annaba University, BP 12-23000 Annaba, Algeria

(Received 16 September 2015; published 29 March 2016)

We report a direct and robust calculation, free from ergodic problems, of the nonuniform-to-uniform (stripe) transition line of noncommutative Φ_2^4 by means of an exact Metropolis algorithm applied to the first nontrivial multitrace correction of this theory on the fuzzy sphere. In fact, we reconstruct the entire phase diagram including the Ising, matrix, and stripe boundaries together with the triple point. We also report that the measured critical exponents of the Ising transition line agrees with the Onsager values in two dimensions. The triple point is identified as a termination point of the one-cut-to-two-cut transition line and is located at $(\tilde{b},\tilde{c}) = (-1.55, 0.4)$, which compares favorably with a previous Monte Carlo estimate.

DOI: 10.1103/PhysRevD.93.065056

I. INTRODUCTION

Noncommutative scalar phi-four theory is a two-parameter model that enjoys three stable phases: (i) disordered (symmetric, one-cut, disk) phase; (ii) uniform ordered (Ising, broken, asymmetric one-cut) phase; and (iii) nonuniform ordered (matrix, stripe, two-cut, annulus) phase. This picture is expected to hold for noncommutative/fuzzy phi-four theory in any dimension, and the three phases are all stable and are expected to meet at a triple point. The nonuniform ordered phase [1] is a full blown nonperturbative manifestation of the perturbative UV-IR mixing effect [2], which is due to the underlying highly nonlocal matrix degrees of freedom of the noncommutative scalar field.

The phase structure in four dimensions was discussed using the Hartree-Fock approximation in [3] and studied by means of the Monte Carlo method, employing the fuzzy torus [4] as regulator, in [5].

In two dimensions the theory is renormalizable [6]. The regularized theory on the fuzzy sphere [7,8] reads

$$S = \mathrm{Tr}(a\Phi[L_a,[L_a,\Phi]] + b\Phi^2 + c\Phi^4). \qquad (1.1)$$

The Laplacian $\Delta = \mathcal{L}_a\mathcal{L}_a$ defines the underlying geometry, i.e., the metric, of the fuzzy sphere in the sense of [9,10]. It is found that the collapsed parameters are

$$\tilde{b} = bN^{-3/2}/a, \qquad \tilde{c} = cN^{-2}/a^2. \qquad (1.2)$$

The above phase structure was confirmed in two dimensions by means of Monte Carlo simulations on the fuzzy sphere in [11,12]. The phase diagram is shown in Fig. 1. Both parts were generated using the Metropolis algorithm on the fuzzy sphere. In the first part coupling of the scalar field Φ to a $U(1)$ gauge field on the fuzzy sphere is included, and as a consequence, we can employ the $U(N)$ gauge symmetry to reduce the scalar sector to only its eigenvalues. In the second part an approximate Metropolis, which does not satisfy detailed balanced, is used.

The problem of the phase structure of fuzzy scalar phi-four was also studied by means of the Monte Carlo method in [13–17]. The analytic derivation of the phase diagram of noncommutative phi-four on the fuzzy sphere was attempted in [18–25]. The related problem of Monte Carlo simulation of noncommutative phi-four on the fuzzy torus and the fuzzy disk was considered in [5], [26], and [27], respectively. For a recent study see [28].

In this paper, we are interested in studying by means of the Monte Carlo method the first nontrivial multitrace matrix model, quartic in the scalar field, which approximates noncommutative Φ^4 on the fuzzy sphere. The multitrace approach was initiated in [18,19]. See also [24] for a review and an extension of this method to the noncommutative Moyal-Weyl plane. For an earlier approach see [25], and for a similar more nonperturbative approach see [20–23]. The multitrace expansion is the analogue of the Hopping parameter expansion on the lattice in the sense that we perform a small kinetic term expansion, i.e. expanding in the parameter a of (1.1), while treating the potential exactly. This should be contrasted with the small interaction expansion of the usual perturbation theory. This technique is expected to capture the matrix transition between disordered and nonuniform ordered phases with arbitrarily increasing accuracy by including more and more terms in the expansion in a. From this we can then infer and/or estimate the position of the triple point. Capturing the Ising transition, and as a consequence the stripe transition, is more subtle and is possible, in our opinion, only if we include odd moments in the effective action and do not impose the symmetry $\Phi \to -\Phi$.

The effective action obtained in the multitrace approach is a multitrace matrix model, depending on various

*ydri@stp.dias.ie

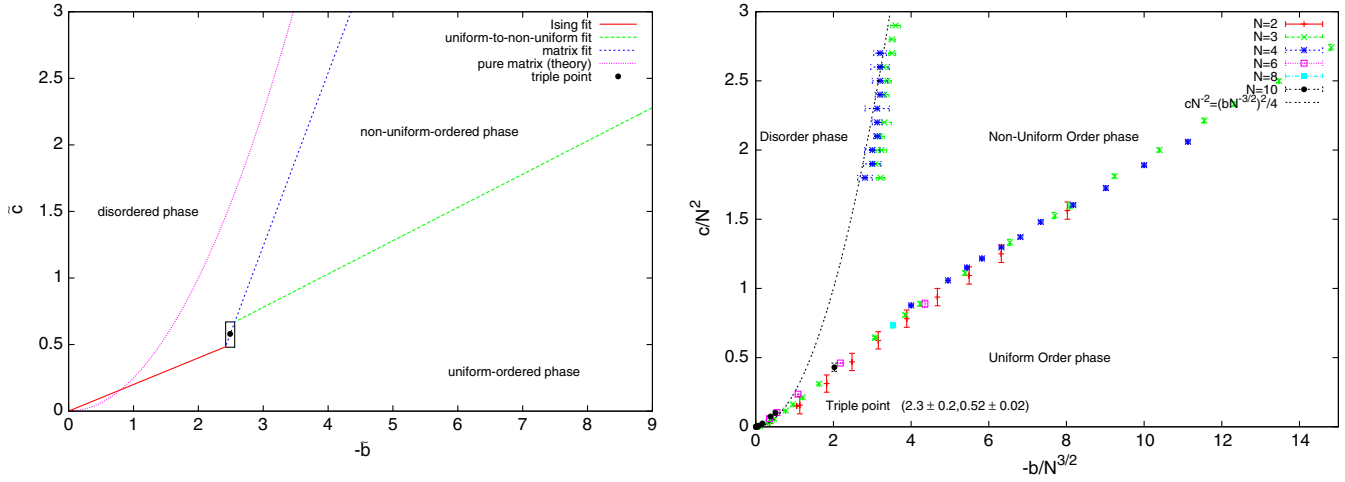

FIG. 1. The phase diagram of noncommutative phi-four theory on the fuzzy sphere. In the first part the fits are reproduced from actual Monte Carlo data [17]. The second part is reproduced from [11] with the gracious permission of D. O'Connor.

moments $m_n = \mathrm{Tr}M^n$ of an $N \times N$ matrix M, which to the lowest nontrivial order is of the form

$$V = B\mathrm{Tr}M^2 + C\mathrm{Tr}M^4 + D[\mathrm{Tr}M^2]^2 + B'(\mathrm{Tr}M)^2 + C'\mathrm{Tr}M\mathrm{Tr}M^3 + D'(\mathrm{Tr}M)^4 + A'\mathrm{Tr}M^2(\mathrm{Tr}M)^2 + \ldots. \quad (1.3)$$

The parameters B and C are shifted values of b and c appearing in (1.1). The primed parameters depend on a. The second line includes terms that depend on the odd moments m_1 and m_3. By diagonalization we obtain therefore the N eigenvalues of M as our independent set of dynamical degrees of freedom with an effective action of the form

$$S_{\mathrm{eff}} = \sum_i (b\lambda_i^2 + c\lambda_i^4) - \frac{1}{2}\sum_{i\neq j}\ln(\lambda_i - \lambda_j)^2 + \left[\frac{r^2}{8}v_{2,1}\sum_{i\neq j}(\lambda_i - \lambda_j)^2 + \frac{r^4}{48}v_{4,1}\sum_{i\neq j}(\lambda_i - \lambda_j)^4 - \frac{r^4}{24N^2}v_{2,2}\left[\sum_{i\neq j}(\lambda_i - \lambda_j)^2\right]^2 + \ldots\right]. \quad (1.4)$$

The coefficients $v_{2,1}$, $v_{4,1}$, and $v_{2,2}$ are given by the following two competing calculations found in [18] (Model I) and [24] (Model II):

$$v_{2,1} = -1, \quad v_{4,1} = \frac{3}{2}, \quad v_{2,2} = 0, \quad \text{Model I}$$
$$v_{2,1} = +1, \quad v_{4,1} = 0, \quad v_{2,2} = \frac{1}{8}, \quad \text{Model II}. \quad (1.5)$$

The result found in [24] agrees with the nonperturbative result of [20] and the corrected result of [19]. This can also be confirmed by means of the Monte Carlo method. The first model in the commutative limit $N \to \infty$ is therefore a scalar Φ^4 theory on the sphere modulo multi-integral terms. In here, we will study both models by means of the Monte Carlo method and show that the first model, though incorrect, sustains the uniform ordered phase. The second model will sustain the uniform ordered phase only if we add to it higher order multitrace corrections.

Since these models depend only on N independent eigenvalues, their Monte Carlo sampling by means of the Metropolis algorithm does not suffer from any ergodic problem and thus what we get in the simulations is really what should exist in the model nonperturbatively. This should be contrasted with the Monte Carlo simulation (via Metropolis, hybrid Monte Carlo, or other method) of (1.1) which suffers from severe ergodic problems that do not allow us easy and transparent access to the stripe transition and the triple point [13–17]. Model I, which sustains the uniform ordered phase, suffers, however, from critical slowing down, for values of N of the order of $N > 60$, and thus the use of the Wolf algorithm [29] would have been more appropriate.

Some of our results in this article include the following:

(i) The phase diagram of Model I contains the three phases discussed above. The critical boundaries are determined, and the triple point is located.

(ii) The uniform ordered phase exists in Model I only with the odd terms included. If we assume the symmetry $M \to -M$, then the second line of (1.3) becomes identically zero and the uniform ordered phase disappears. This is at least true in the domain studied in this article, which includes the triple point of fuzzy Φ^4 on the fuzzy sphere and extends to all its phase diagrams probed in [11,12].

(iii) The delicate computation of the critical exponents of the Ising transition is discussed, and our estimate of the critical exponents ν, α, γ, β agrees very well with the Onsager values [30].

(iv) The phase diagram of Model II, with or without odd terms, does not contain the uniform ordered phase.
(v) The one-cut-to-two-cut transition line does not extend to the origin, i.e. to $\tilde{C} = 0$, in Model II, which gives us an estimation of the triple point in this case.
(vi) In Model II without the odd terms the termination point can be computed analytically from the requirement that the critical point $\tilde{B}_*$ always remains negative and the obtained result $(\tilde{B}, \tilde{C}) = (0, 1/12)$ agrees with the Monte Carlo method.
(vii) In Model II with odd terms the termination point is found to be located at $(\tilde{B}, \tilde{C}) = (-1.05, 0.4)$. This is our measurement of the triple point.
(viii) In all cases the one-cut-to-two-cut matrix transition line agrees better with the double-trace matrix theory than with the quartic matrix model. The double-trace matrix theory is given by $D \neq 0$ while all primed parameters are zero.
(ix) The model of Grosse-Wulkenhaar is also briefly discussed.

This article is organized as follows:

(1) Section 2: The Multitrace Matrix Models.
(2) Section 3: Exact Solutions.
  (a) The Pure Real Quartic Matrix Model.
  (b) The Double-trace Quartic Matrix Model.
(3) Section 4: Algorithm.
(4) Section 5: Monte Carlo Results.
  (a) General Remarks.
  (b) Monte Carlo Tests of Multitrace Approximations.
  (c) Phase Diagrams.
  (d) Gross-Wulkenhaar Model.
(5) Section 5: Conclusion.

We also include appendixes for the benefit of interested readers as well as to make the presentation as self-contained as possible.

II. THE MULTITRACE MATRIX MODELS

Our primary interest here is the theory of noncommutative Φ^4 on the fuzzy sphere given by the action

$$S = \frac{4\pi R^2}{N+1} \mathrm{Tr}\left(\frac{1}{2R^2}\Phi\Delta\Phi + \frac{1}{2}m^2\Phi^2 + \frac{\lambda}{4!}\Phi^4\right). \quad (2.1)$$

The Laplacian is $\Delta = [L_a, [L_a, \ldots]]$. Equivalently with the substitution $\Phi = \mathcal{M}/\sqrt{2\pi\theta}$, where $\mathcal{M} = \sum_{i,j=1}^{N} M_{ij}|i\rangle\langle j|$, this action reads

$$S = \mathrm{Tr}(a\mathcal{M}\Delta\mathcal{M} + b\mathcal{M}^2 + c\mathcal{M}^4). \quad (2.2)$$

The parameters are[1]

$$a = \frac{1}{2R^2}, \qquad b = \frac{1}{2}m^2, \qquad c = \frac{\lambda}{4!}\frac{1}{2\pi\theta}. \quad (2.3)$$

In terms of the matrix M the action reads

$$S[M] = r^2 K[M] + \mathrm{Tr}[bM^2 + cM^4]. \quad (2.4)$$

The kinetic matrix is given by

$$K[M] = \mathrm{Tr}\left[-\Gamma^+ M\Gamma M - \frac{1}{N+1}\Gamma_3 M\Gamma_3 M + EM^2\right]. \quad (2.5)$$

The matrices Γ, Γ_3, and E are given by

$$(\Gamma_3)_{lm} = l\delta_{lm}, \qquad (\Gamma)_{lm} = \sqrt{(m-1)\left(1 - \frac{m}{N+1}\right)}\delta_{lm-1},$$
$$(E)_{lm} = \left(l - \frac{1}{2}\right)\delta_{lm}. \quad (2.6)$$

The relationship between the parameters a and r^2 is given by

$$r^2 = 2aN. \quad (2.7)$$

We start from the path integral

$$\begin{aligned} Z &= \int dM \exp(-S[M]) \\ &= \int d\Lambda \Delta^2(\Lambda) \exp(-\mathrm{Tr}(b\Lambda^2 + c\Lambda^4)) \\ &\quad \times \int dU \exp(-r^2 K[U\Lambda U^{-1}]). \end{aligned} \quad (2.8)$$

The second line involves the diagonalization of the matrix M (more on this below). The calculation of the integral over $U \in U(N)$ is a very long calculation done in [18,24]. The end result is a multitrace effective potential given by

$$\begin{aligned} S_{\mathrm{eff}} &= \sum_i (b\lambda_i^2 + c\lambda_i^4) - \frac{1}{2}\sum_{i\neq j} \ln(\lambda_i - \lambda_j)^2 \\ &\quad + \left[\frac{r^2}{8} v_{2,1} \sum_{i\neq j} (\lambda_i - \lambda_j)^2 + \frac{r^4}{48} v_{4,1} \sum_{i\neq j} (\lambda_i - \lambda_j)^4 \right. \\ &\quad \left. - \frac{r^4}{24N^2} v_{2,2} \left[\sum_{i\neq j} (\lambda_i - \lambda_j)^2\right]^2 + \ldots\right]. \end{aligned} \quad (2.9)$$

The coefficients v will be given below.

We will assume now that the parameters b, c, and r^2 scale as

$$\tilde{a} = \frac{a}{N^{\delta_a}}, \quad \tilde{b} = \frac{b}{N^{\delta_b}}, \quad \tilde{c} = \frac{c}{N^{\delta_c}}, \quad \tilde{r}^2 = \frac{r^2}{N^{\delta_r}}. \quad (2.10)$$

Further, we will assume a scaling δ_λ of the eigenvalues λ, viz.

[1]The noncommutativity parameter on the fuzzy sphere is related to the radius of the sphere by $\theta = 2R^2/\sqrt{N^2-1}$.

$$\tilde{\lambda} = \frac{\lambda}{N^{\delta_\lambda}}. \tag{2.11}$$

It is easy to convince ourselves that in order for the above effective potential to come out of order N^2 we must have the following values:

$$\delta_a = -1-2\delta_\lambda, \quad \delta_b = 1-2\delta_\lambda, \quad \delta_c = 1-4\delta_\lambda, \quad \delta_r = -2\delta_\lambda. \tag{2.12}$$

From the Monte Carlo results of [11,12], we know that the scaling behavior of the parameters b and c appearing in the above action on the fuzzy sphere is given by

$$\delta_b = \frac{3}{2}, \qquad \delta_c = 2. \tag{2.13}$$

By substitution we obtain the other scalings

$$\delta_\lambda = -\frac{1}{4}, \qquad \delta_a = -\frac{1}{2}, \qquad \delta_r = \frac{1}{2}. \tag{2.14}$$

The problem (2.9) is a generalization of the quartic Hermitian matrix potential model. Indeed, by dropping odd moments, this effective potential corresponds to the matrix model given by

$$V = V_0 + \Delta V_0. \tag{2.15}$$

The classical potential and the even correction ΔV_0 are given by

$$V_0 = b\mathrm{Tr}M^2 + c\mathrm{Tr}M^4, \tag{2.16}$$

$$\Delta V_0 = F'\mathrm{Tr}M^2 + E'\mathrm{Tr}M^4 + D[\mathrm{Tr}M^2]^2. \tag{2.17}$$

The coefficients F', E', and D are given by

$$F' = \frac{aN^2 v_{2,1}}{2}, \qquad E' = \frac{a^2N^3 v_{4,1}}{6}, \qquad D = -\frac{2\eta a^2 N^2}{3}. \tag{2.18}$$

The strength of the multitrace term η is given by

$$\eta = v_{2,2} - \frac{3}{4}v_{4,1}. \tag{2.19}$$

By including terms that involve the odd moments we get the effective potential

$$V = V_0 + \Delta V_0 + \Delta V. \tag{2.20}$$

The extra contribution and its coefficients are given by

$$\Delta V = B'(\mathrm{Tr}M)^2 + C'\mathrm{Tr}M\mathrm{Tr}M^3 + D'(\mathrm{Tr}M)^4 + A'\mathrm{Tr}M^2(\mathrm{Tr}M)^2, \tag{2.21}$$

$$B' = -\frac{aN}{2}v_{2,1}, \qquad C' = -\frac{2a^2N^2}{3}v_{4,1},$$
$$D' = -\frac{2a^2}{3}v_{2,2}, \qquad A' = \frac{4a^2N}{3}v_{2,2}. \tag{2.22}$$

The coefficients $v_{2,1}$, $v_{4,1}$, and $v_{2,2}$ are given by the following two competing calculations found in [18] (Model I) and [24] (Model II):

$$v_{2,1} = -1, \quad v_{4,1} = \frac{3}{2}, \quad v_{2,2} = 0, \quad \text{Model I}$$
$$v_{2,1} = +1, \quad v_{4,1} = 0, \quad v_{2,2} = \frac{1}{8}, \quad \text{Model II}. \tag{2.23}$$

The difference in the sign of $v_{2,1}$ is probably a typo on the part of [18] while the discrepancy in the values of $v_{4,1}$ and $v_{2,2}$ is more serious and is discussed in [24]. The result found in [24] agrees with the result of [20] given by their Eq. (2.39). The work [19] contains the correct calculation, which agrees with the results of both [20] and [24].

The one-cut-to-two-cut transition line in the model (2.15) is given by the exact result [24]

$$\tilde{b}_* = -\frac{\tilde{a}}{2}v_{2,1} - 2\sqrt{\tilde{c} + \frac{\tilde{a}^2}{6}v_{4,1}} + \frac{4\eta\tilde{a}^2}{3\sqrt{\tilde{c} + \frac{\tilde{a}^2}{6}v_{4,1}}}. \tag{2.24}$$

As pointed out in [24] this result is new. For a generalization of this result see [20]. This critical value $\tilde{b}_*$ is negative for

$$\tilde{c} \geq \frac{\tilde{a}^2}{6}(4\eta - v_{4,1}). \tag{2.25}$$

III. EXACT SOLUTIONS

In this section we will give a brief description of the exact solutions of the real quartic matrix model $B\mathrm{Tr}M^2 + C\mathrm{Tr}M^4$ and the double-trace real quartic matrix model $B\mathrm{Tr}M^2 + C\mathrm{Tr}M^4 + D(\mathrm{Tr}M^2)^2$.

A. The pure real quartic matrix model

The phase structure of the pure real quartic matrix model is studied, for example, in [31–34]. In here we will summarize some of the salient results.

The basic model is given by

$$V = B\mathrm{Tr}M^2 + C\mathrm{Tr}M^4 = \frac{N}{g}\left(-\mathrm{Tr}M^2 + \frac{1}{4}\mathrm{Tr}M^4\right), \tag{3.1}$$

$$B = -\frac{N}{g}, \qquad C = \frac{N}{4g}. \tag{3.2}$$

There are two phases in this case:

Disordered phase (one-cut) for $g \geq g_c$:

$$\rho(\lambda) = \frac{1}{N\pi}(2C\lambda^2 + B + C\delta^2)\sqrt{\delta^2 - \lambda^2} = \frac{1}{g\pi}\left(\frac{1}{2}\lambda^2 - 1 + r^2\right)\sqrt{4r^2 - \lambda^2} \tag{3.3}$$

$$-2r \leq \lambda \leq 2r, \tag{3.4}$$

$$r = \frac{1}{2}\delta, \tag{3.5}$$

$$\delta^2 = \frac{1}{3C}(-B + \sqrt{B^2 + 12NC}) = \frac{1}{3}(1 + \sqrt{1 + 3g}). \tag{3.6}$$

Nonuniform ordered phase (two-cut) for $g \leq g_c$:

$$\rho(\lambda) = \frac{2C|\lambda|}{N\pi}\sqrt{(\lambda^2 - \delta_1^2)(\delta_2^2 - \lambda^2)} = \frac{|\lambda|}{2g\pi}\sqrt{(\lambda^2 - r_-^2)(r_+^2 - \lambda^2)}, \tag{3.7}$$

$$r_- \leq |\lambda| \leq r_+, \tag{3.8}$$

$$r_- = \delta_1, \qquad r_+ = \delta_2, \tag{3.9}$$

$$r_\mp^2 = \frac{1}{2C}(-B \mp 2\sqrt{NC}) = 2(1 \mp \sqrt{g}). \tag{3.10}$$

Critical point: A third order transition between the above two phases occurs at the critical point

$$g_c = 1 \leftrightarrow B_c^2 = 4NC \leftrightarrow B_c = -2\sqrt{NC}. \tag{3.11}$$

Specific heat: The behavior of the specific heat across the matrix transition provides also a powerful result against which we can calibrate our algorithms and Monte Carlo simulations. In terms of $\bar{B} = B/B_c$ the specific heat reads in the two phases of the theory as follows:

$$\frac{C_v}{N^2} = \frac{1}{4}, \qquad \bar{B} = B/B_c < -1,$$
$$\frac{C_v}{N^2} = \frac{1}{4} + \frac{2\bar{B}^4}{27} - \frac{\bar{B}}{27}(2\bar{B}^2 - 3)\sqrt{\bar{B}^2 + 3}, \qquad \bar{B} > -1. \tag{3.12}$$

Uniform ordered phase: The real quartic matrix model admits also a solution with $\mathrm{Tr}M \neq 0$ corresponding to a possible uniform-ordered (Ising) phase. This $U(N)$-like solution can appear only for negative values of the mass parameter μ, and it is constructed, for example, in [31]. It is, however, thought that this solution cannot yield to a stable phase without the addition of the kinetic term to the real quartic matrix model.

The density of eigenvalues in this case is given by

$$\rho(z) = \frac{1}{\pi N}(2Cz^2 + 2\sigma Cz + B + 2C\sigma^2 + C\tau^2) \times \sqrt{((\sigma + \tau) - z)(z - (\sigma - \tau))}. \tag{3.13}$$

This is a one-cut solution centered around τ in the interval $[\sigma - \tau, \sigma + \tau]$ where σ and τ are given by

$$\sigma^2 = \frac{1}{10C}(-3B + 2\sqrt{B^2 - 15NC}),$$
$$\tau^2 = \frac{1}{15C}(-2B - 2\sqrt{B^2 - 15NC}). \tag{3.14}$$

This solution makes sense only for

$$B \leq B_c = -\sqrt{15}\sqrt{NC}. \tag{3.15}$$

B. The double-trace quartic matrix model

The double-trace real quartic matrix model is given by the multitrace matrix model (1.3) with all odd moments set to zero, viz.

$$V = B\mathrm{Tr}M^2 + C\mathrm{Tr}M^4 + D(\mathrm{Tr}M^2)^2. \tag{3.16}$$

The scaling of the parameters is given by

$$\tilde{B} = BN^{-3/2}, \qquad \tilde{C} = CN^{-2}, \qquad \tilde{D} = DN^{-1}. \tag{3.17}$$

The phase structure of this model is very similar to the phase structure of the pure real quartic matrix model outlined in the previous section. See, for example, [24]. The two stable phases are still given by the disordered (one-cut) phase and the nonuniform-ordered (two-cut) phase separated by a deformation of the line $\tilde{B}_* = -2\sqrt{\tilde{C}}$ given by

$$\tilde{B}_* = -2\sqrt{\tilde{C}} - \frac{2\tilde{D}}{\sqrt{\tilde{C}}}. \tag{3.18}$$

For a generalization of this result see [20].

Another important result for us here is the existence of a termination point in the model of [24] since the critical line does not extend to zero. Indeed, in order for the critical value $\tilde{B}_*$ to be negative, one must have $\tilde{C}$ in the range

$$\tilde{C} \geq \tilde{C}_* = \frac{2\eta\tilde{a}^2}{3} = \frac{\tilde{a}^2}{12}. \tag{3.19}$$

Thus the termination point is located at (for $\tilde{a} = 1$)

$$(\tilde{B}, \tilde{C}) = (0, 1/12). \tag{3.20}$$

IV. ALGORITHM

We start from the potential and the partition function

$$V = \mathrm{Tr}(BM^2 + CM^4) + D(\mathrm{Tr}M^2)^2 + B'(\mathrm{Tr}M)^2 + C'\mathrm{Tr}M\mathrm{Tr}M^3 + D'(\mathrm{Tr}M)^4 + A'\mathrm{Tr}M^2(\mathrm{Tr}M)^2, \tag{4.1}$$

$$Z = \int dM \exp(-V). \tag{4.2}$$

The relationship between the two sets of parameters $\{a, b, c\}$ and $\{B, C, D\}$ is given by

$$B = b + \frac{aN^2 v_{2,1}}{2}, \quad C = c + \frac{a^2N^3 v_{4,1}}{6}, \quad D = -\frac{2\eta a^2 N^2}{3}. \tag{4.3}$$

The collapsed parameters are

$$\tilde{B} = \frac{B}{N^{\frac{3}{2}}} = \tilde{b} + \frac{\tilde{a}v_{2,1}}{2}, \qquad \tilde{C} = \frac{C}{N^2} = \tilde{c} + \frac{\tilde{a}^2 v_{4,1}}{6},$$
$$D = -\frac{2\eta\tilde{a}^2 N}{3}. \tag{4.4}$$

Only two of these three parameters are independent. For consistency of the large N limit, we must choose $\tilde{a}$ to be any fixed number. We then choose for simplicity $\tilde{a} = 1$ or equivalently $D = -2\eta N/3$.[2] The other parameters are

$$B' = -\frac{aN}{2} v_{2,1}, \qquad C' = -\frac{2a^2N^2}{3} v_{4,1},$$
$$D' = -\frac{2a^2}{3} v_{2,2}, \qquad A' = \frac{4a^2N}{3} v_{2,2}. \tag{4.5}$$

We can now diagonalize the scalar matrix M as

$$M = U\Lambda U^{-1}. \tag{4.6}$$

We compute

$$\delta M = U(\delta\Lambda + [U^{-1}\delta U, \Lambda])U^{-1}. \tag{4.7}$$

Thus [with $U^{-1}\delta U = i\delta V$ being an element of the Lie algebra of SU(N)]

$$\mathrm{Tr}(\delta M)^2 = \mathrm{Tr}(\delta\Lambda)^2 + \mathrm{Tr}[U^{-1}\delta U, \Lambda]^2 = \sum_i (\delta\lambda_i)^2 + \sum_{i\neq j}(\lambda_i - \lambda_j)^2 \delta V_{ij}\delta V^*_{ij}. \tag{4.8}$$

We count N^2 real degrees of freedom as there should be. The measure is therefore given by

$$dM = \prod_i d\lambda_i \prod_{i\neq j} dV_{ij} dV^*_{ij} \sqrt{\det(\mathrm{metric})} = \prod_i d\lambda_i \prod_{i\neq j} dV_{ij} dV^*_{ij} \sqrt{\prod_{i\neq j}(\lambda_i - \lambda_j)^2}. \tag{4.9}$$

We write this as

$$dM = d\Lambda dU \Delta^2(\Lambda). \tag{4.10}$$

The dU is the usual Haar measure over the group SU(N) which is normalized such that $\int dU = 1$, whereas the Jacobian $\Delta^2(\Lambda)$ is precisely the so-called Vandermonde determinant defined by

$$\Delta^2(\Lambda) = \prod_{i>j}(\lambda_i - \lambda_j)^2. \tag{4.11}$$

The partition function becomes

$$Z = \int d\Lambda \Delta^2(\Lambda) \exp(-\mathrm{Tr}(B\Lambda^2 + C\Lambda^4) - D(\mathrm{Tr}\Lambda^2)^2). \tag{4.12}$$

We are therefore dealing with an effective potential given by

$$V_{\mathrm{eff}} = B\sum_{i=1}\lambda_i^2 + C\sum_{i=1}\lambda_i^4 + D\left(\sum_{i=1}\lambda_i^2\right)^2 - \frac{1}{2}\sum_{i\neq j}\ln(\lambda_i - \lambda_j)^2. \tag{4.13}$$

We will use the Metropolis algorithm to study this model. Under the change $\lambda_i \to \lambda_i + h$ of the eigenvalue λ_i the above effective potential changes as $V_{\mathrm{eff}} \to V_{\mathrm{eff}} + \Delta V_{i,h}$ where

$$\Delta V_{i,h} = B\Delta S_2 + C\Delta S_4 + D(2S_2\Delta S_2 + \Delta S_2^2) + \Delta S_{\mathrm{Vand}} + B'\Delta S'_2 + C'\Delta S'_4 + D'((\Delta S'_2)^2 + 2S_1^2\Delta S'_2) + A'((S_1 + h)\Delta S_2 + hS_2). \tag{4.14}$$

The monomials S_n are defined by $S_n = \sum_i \lambda_i^n$ while the variations ΔS_n and ΔS_{Vand} are given by

$$\Delta S_2 = h^2 + 2h\lambda_i, \tag{4.15}$$

$$\Delta S_4 = 6h^2\lambda_i^2 + 4h\lambda_i^3 + 4h^3\lambda_i + h^4, \tag{4.16}$$

$$\Delta S_{\mathrm{Vand}} = -2\sum_{j\neq i}\ln\left|1 + \frac{h}{\lambda_i - \lambda_j}\right|, \tag{4.17}$$

$$\Delta S'_2 = h^2 + 2hS_1, \tag{4.18}$$

$$\Delta S'_4 = (S_1 + h)(3h\lambda_i^2 + 3h^2\lambda_i + h^3) + hS_3. \tag{4.19}$$

[2]The authors of [11,12] chose instead $a = 1$. This should not make any difference to the Monte Carlo simulations.

V. MONTE CARLO RESULTS

A. General remarks

(1) We use the statistics $2^P + 2^P \times 2^{P'}$ with $P = 15$–20 and $P' = 5$ with $N = 10$–60 and with the jackknife method to estimate the error bars. We can even go further to $N = 100$ and beyond but noticed that critical slowing down became a serious obstacle especially in the measurement of critical exponents.

(2) Our first test for the validity of our simulations is to look at the Schwinger-Dyson identity given for the full multitrace model (2.20) by

$$\langle (2b\mathrm{Tr}M^2 + 4c\mathrm{Tr}M^4 + 2V_2 + 4V_4)\rangle = N^2. \quad (5.1)$$

The quartic and quadratic pieces V_2 and V_4 are such that

$$\Delta V_0 + \Delta V = V_2 + V_4. \quad (5.2)$$

In other words,

$$V_2 = F'\mathrm{Tr}M^2 + B'(\mathrm{Tr}M)^2, \quad (5.3)$$

$$V_4 = E'\mathrm{Tr}M^4 + D[\mathrm{Tr}M^2]^2 + C'\mathrm{Tr}M\mathrm{Tr}M^3 + D'(\mathrm{Tr}M)^4 + A'\mathrm{Tr}M^2(\mathrm{Tr}M)^2. \quad (5.4)$$

(3) The second powerful test is to look at the conventional quartic matrix model with $a = 0$, viz. $V = V_0$. The eigenvalues distributions in the two stable phases [disorder(one-cut) and nonuniform order (two-cut)] as well as the demarcation of their boundary are well known analytically given by the formulas (3.3), (3.7), and (3.11).

(4) Even the quartic multitrace approximation itself can be verified directly in Monte Carlo simulation in order to resolve the ambiguity in the coefficients v between [24] and [18]. We must have as identity the two equations

$$\left\langle a\int dU\mathrm{Tr}[L_a, U\Lambda U^{-1}]^2\right\rangle_{V_0} = \langle -V_2(\Lambda)\rangle_{V_0}, \quad (5.5)$$

$$\left\langle \frac{1}{2}\left(a\int dU\mathrm{Tr}[L_a, U\Lambda U^{-1}]^2\right)^2\right\rangle_{V_0} = \left\langle -V_4(\Lambda) + \frac{1}{2}V_2^2(\Lambda)\right\rangle_{V_0}. \quad (5.6)$$

The coefficients v appear in the potentials V_2 and V_4. The expectation values are computed with respect to the conventional quartic matrix model $V_0 = V_0(\Lambda)$.

This test clearly requires the computation of the kinetic term and its square, which means in particular that we need to numerically perform the integral over U in the term $\int dU\mathrm{Tr}[L_a, U\Lambda U^{-1}]^2$, and it is not obvious how to do this in any direct way. Equivalently, we can undo the diagonalization in the terms involving the kinetic term to obtain instead the equations

$$\langle a\mathrm{Tr}[L_a, M]^2\rangle_{V_0} = \langle -V_2\rangle_{V_0}, \quad (5.7)$$

$$\left\langle \frac{1}{2}(a\mathrm{Tr}[L_a, M]^2)^2\right\rangle_{V_0} = \left\langle -V_4 + \frac{1}{2}V_2^2\right\rangle_{V_0}. \quad (5.8)$$

Now the expectation values in the left hand side must be computed with respect to the conventional quartic matrix model $V_0 = V_0(M)$ with the full matrix $M = U\Lambda U^{-1}$ instead of the eigenvalues matrix Λ. The expectation values in the right hand side can be computed either way.

In other words, the eigenvalues Metropolis algorithm employed in this article to compute terms such as $\langle -V_2\rangle_{V_0}$ and $\langle -V_4 + V_2^2/2\rangle_{V_0}$ cannot be used to compute the terms $\langle a\mathrm{Tr}[L_a, M]^2\rangle_{V_0}$ and $\langle a\mathrm{Tr}[L_a, M]^2)^2/2\rangle_{V_0}$. We use instead the hybrid Monte Carlo algorithm to compute these terms as well as the terms $\langle -V_2\rangle_{V_0}$ and $\langle -V_4 + V_2^2/2\rangle_{V_0}$ in order to verify the above equations. This also should be viewed as a countercheck for the hybrid Monte Carlo algorithm[3] since we can compare the values of $\langle -V_2\rangle_{V_0}$ and $\langle -V_4 + V_2^2/2\rangle_{V_0}$ obtained using the hybrid Monte Carlo algorithm with those obtained using our eigenvalues Metropolis algorithm. We note, in passing, that the Metropolis algorithm employed for the eigenvalues problem here is far more efficient than the hybrid Monte Carlo algorithm applied to the same problem without diagonalization. But this we can obviously tolerate for testing purposes.

(5) The most detailed order parameter at our disposal is the eigenvalues distribution of the field/matrix M, which behaves in distinct ways in various phases. This behavior mimics their behavior in the conventional quartic matrix model V_0, viz.
   (a) The disorder (one-cut) phase is characterized by a single-cut eigenvalues distribution symmetric around 0 since in this phase $\langle M\rangle = 0$.
   (b) The nonuniform order (two-cut) phase is characterized by an eigenvalues distribution symmetric around 0 but with two disjoint supports since $\langle M\rangle = \sqrt{-b/2c}\gamma$ where γ is any

[3]Or a countercheck for the eigenvalues Metropolis algorithm depending on which algorithm is more trustworthy. However, we firmly believe that the eigenvalues Metropolis algorithm used here is more robust on all accounts.

N-dimensional idempotent, i.e. $\gamma^2 = 1$. This appears for large values of $\tilde{c}$.

(c) The uniform order (asymmetric one-cut) phase is characterized by a single-cut eigenvalues distribution centered around a nonzero value since $\langle M \rangle = \sqrt{-b/2c}\mathbf{1}$. This appears for small values of $\tilde{c}$.

(6) The specific heat defined with the respect to the multitrace potential is given by

$$C_v = \langle V^2 \rangle - \langle V \rangle^2. \tag{5.9}$$

The relation of this powerful and most difficult to measure second moment with the specific heat of noncommutative Φ^4 on the fuzzy sphere is discussed in the Appendix. In any case, this specific heat is expected to approach the specific heat of the original noncommutative Φ^4 for large values of $\tilde{c}$, and as a consequence it can be used to locate the boundary between one-cut and two-cut phases as in the conventional quartic matrix model with $a = 0$.

(7) The magnetization and susceptibility are defined by

$$m = \langle |\mathrm{Tr}M| \rangle, \quad \chi = \langle |\mathrm{Tr}M|^2 \rangle - \langle |\mathrm{Tr}M| \rangle^2. \tag{5.10}$$

The magnetic susceptibility will exhibit peaks in the second order phase transitions between disorder (one-cut) and uniform order (Ising) and between nonuniform order (two-cut) and uniform order (Ising).

(8) The total power and power in the zero mode are defined by

$$P_T = \left\langle \frac{1}{N}\mathrm{Tr}M^2 \right\rangle, \quad P_0 = \left\langle \left(\frac{1}{N}\mathrm{Tr}M\right)^2 \right\rangle. \tag{5.11}$$

In the Ising (uniform order) phase we will have in particular the very distinguished signal $P = P_0$.

B. Monte Carlo tests of multitrace approximations

It is quite obvious that resolving the ambiguity between the calculations of [18] and [24], summarized in Eq. (2.23), is straightforward in Monte Carlo tests. We only need to show that the two equations (5.7) and (5.8) hold as identities in the correct calculation. However, this requires a different algorithm than the eigenvalues Metropolis algorithm used here. Indeed, to solve this problem we need to Monte Carlo sample both the eigenvalues and the angles of the matrix M using the Metropolis or the hybrid Monte Carlo algorithm, the quartic matrix model

$$V_0 = b\mathrm{Tr}M^2 + c\mathrm{Tr}M^4. \tag{5.12}$$

Monte Carlo simulations of this model can also be compared to the exact solution outlined in Sec. III. A so calibration in this case is easy. The detail of this simple exercise is reported in [24]. There, it is decisively shown that the calculation of [24] gives the correct approximation of noncommutative scalar Φ_2^4 on the fuzzy sphere.

C. Phase diagrams

(1) *Model I*: *Model of* [18]:

(a) *Ising*: Some of the results for the Ising transition for this model are shown in Table I. The critical point is taken at the peak of the susceptibility. The behavior of various observables is shown in Fig. 2. The fit for the extrapolated critical value is given by

$$\tilde{C} = 0.291(0) \cdot (-\tilde{B}) + 0.104(1). \tag{5.13}$$

This transition can be confirmed to be between disordered and uniform-ordered by looking at the eigenvalues distribution. In the disordered phase we have one-cut symmetric around zero, whereas in the uniform-ordered we have one-cut symmetric around $\sqrt{-B/2C}$. See Fig. 3.

(b) *Critical exponents*: The calculation of the critical exponents of the above Ising transition is a very delicate exercise in Monte Carlo simulation due to the known problem of critical slowing down, and as a consequence the use of a different algorithm, for large values of N, such as the Wolf algorithm [29] is essential. For values of N less than $N = 60$ the current algorithm is sufficient. In any case, this lengthy calculation is reported elsewhere. Suffice it to say here that the critical exponents obtained are consistent, within the best statistical errors, with the Onsager solution of the Ising model in two dimensions given by the celebrated values [30]

$$\nu = 1, \quad \beta = 1/8, \quad \gamma = 7/4, \quad \alpha = 0, \quad \eta = 1/4. \tag{5.14}$$

This has always been known to be true, but this is the first Monte Carlo direct calculation of these critical exponents.

(c) *Matrix:* Some of the results for the matrix transition between disorder and nonuniform order for this model are shown in Table II. The critical point is determined at the point

TABLE I. The Ising transition points for $N = 10$–50. These are determined at the peak of the susceptibility (discontinuity in the specific heat). The search step is 0.01.

$\tilde{C}$	$N = 10$	$N = 25$	$N = 36$	$N = 50$	$\tilde{B}$ extrapolated
0.3	−0.71	−0.69	−0.68	−0.68	−0.672(2)
0.5	−1.44	−1.39	−1.38	−1.38	−1.361(3)
1.0	−3.21	−3.13	−3.11	−3.10	−3.073(2)
1.2	−3.9	−3.82	−3.8	−3.79	−3.763(2)

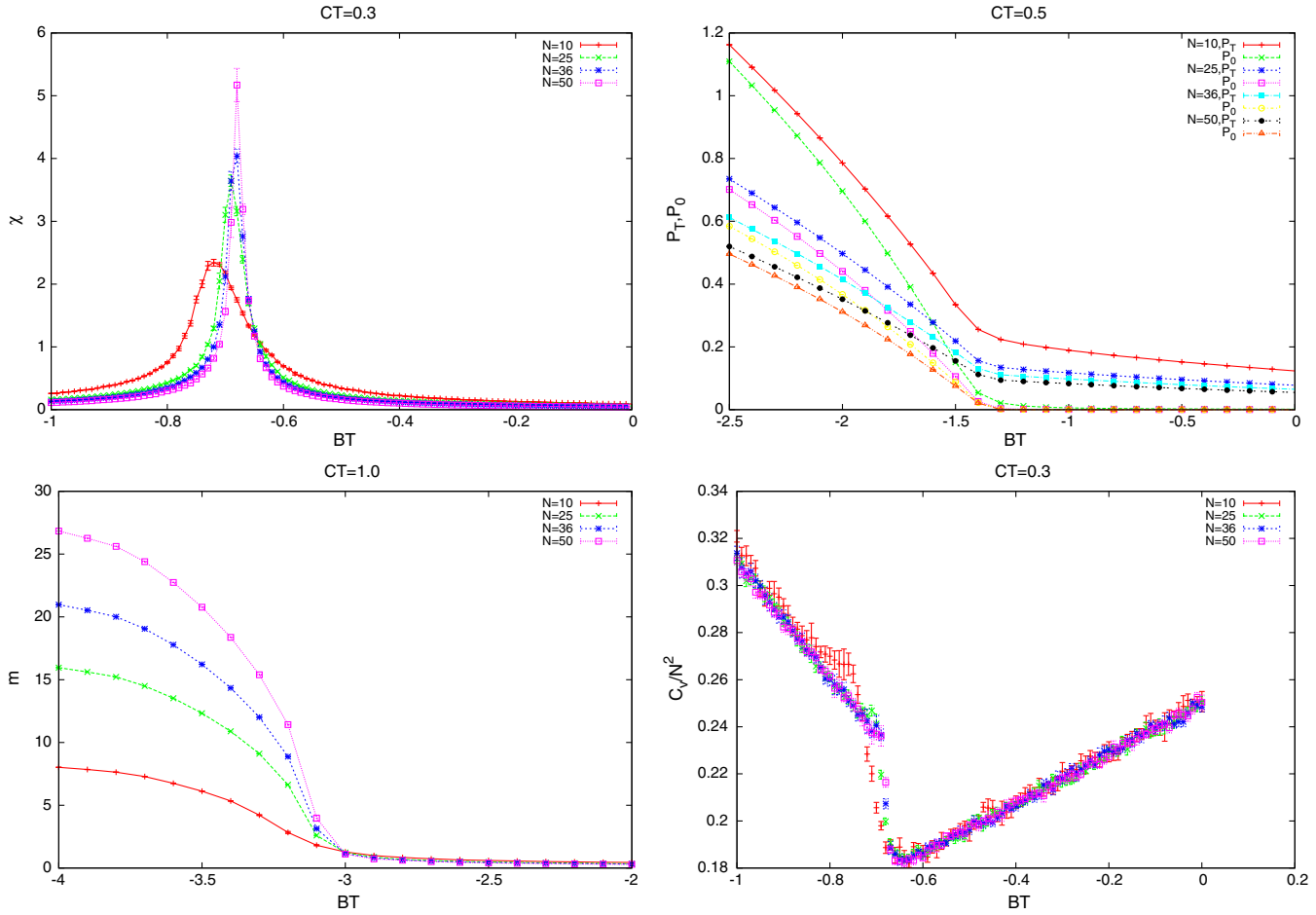

FIG. 2. Some observables of the multitrace model of [18] across the disorder-to-uniform transition.

where the eigenvalue distributions go from one-cut in the disorder phase to two-cut in the nonuniform phase. The splitting of the distribution is considered to have occurred when the height of the distribution at $\lambda = 0$ is less than some tolerance Tol. We take Tol $= 0.001$. The behavior of the specific heat across this transition is effectively that of the pure quartic matrix model $a = 0$. A sample of the corresponding specific heats and eigenvalue distributions is shown in Fig. 4. The fit for the extrapolated critical value is given by

$$\tilde{C} = 2.206(67) \cdot (-\tilde{B}) - 7.039(301). \qquad (5.15)$$

(d) *Stripe:* This transition is quite difficult to observe in Monte Carlo simulation even in this simplified setting that involves the sampling of N eigenvalues. We can observe this transition for medium values of $\tilde{C}$ immediately above, but not too close to, the triple point. The transition point is taken at the point where we observe a jump or a discontinuity in the zero power P_0 and the specific heat as seen in Fig. 5.

Alternatively, we can approach the critical boundary by fixing the value of $\tilde{B}$ and changing $\tilde{C}$ starting from small values, i.e. inside the uniform ordered phase, until the curves for the total and zero powers start to diverge marking the transition to the nonuniform ordered phase. The signal we obtain in this way is quite clear and unambiguous as shown in Fig. 6, and some measurements are included in Table III. Since this is a very delicate transition, we do not perform any extrapolation of the critical point, and the critical boundary is given by the fit of the largest value of N. In any case we observe no strong dependence on N of the measured critical value $\tilde{C}$ as seen in Table III. The stripe critical line is then approximated by the fit for $N = 50$ given by

$$\tilde{C} = 0.154(22) \cdot (-\tilde{B}) + 0.530(131), \qquad N = 50. \qquad (5.16)$$

(e) *Triple point and phase diagram:* The location of the triple point is obtained from the intersection point of the Ising and matrix lines (5.13)

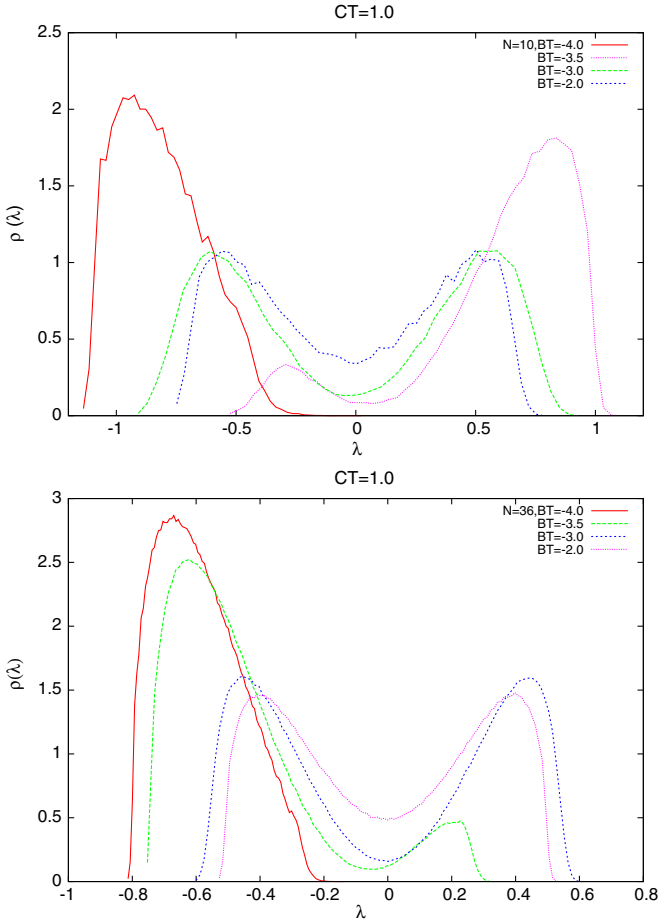

FIG. 3. The eigenvalues distribution of the matrix M in the multitrace model of [18] with $\tilde{C} = 1.0$ across the disorder-to-uniform transition.

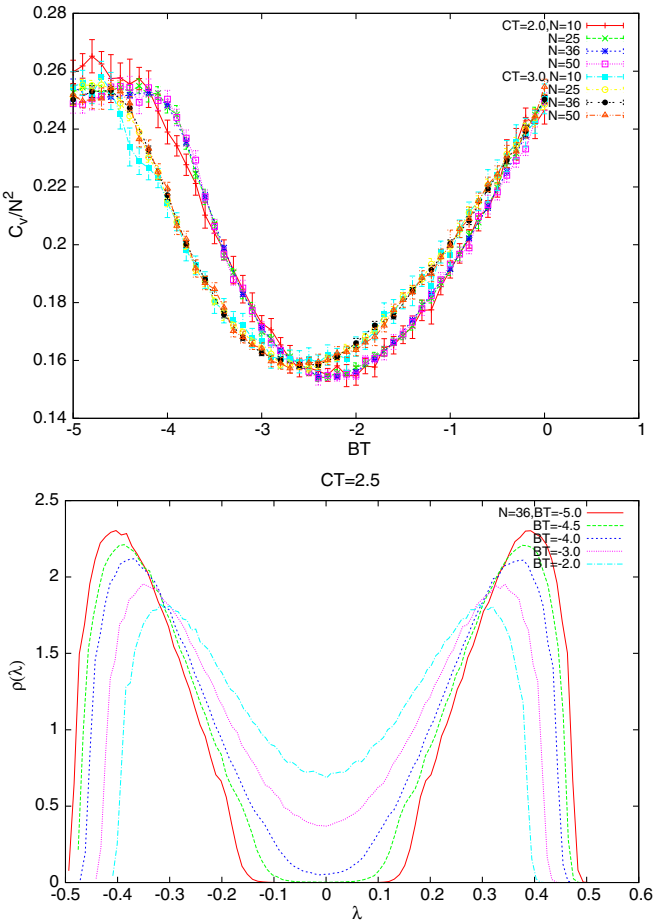

FIG. 4. The specific heat and the eigenvalues distribution of the matrix M in the multitrace model of [18] across the disorder-to-nonuniform transition.

and (5.15), respectively. Indeed, the measurement of these two lines is more robust than the measurement of the stripe line (5.16). We get then immediately

$$(\tilde{B}, \tilde{C}) = (-3.73, 1.19). \tag{5.17}$$

The phase diagram of the multitrace model of [18] is shown in Fig. 7. The Ising and matrix transition data points are not shown explicitly, but we only include their extrapolated fits, whereas the $N = 50$, 36, and 25 stripe data points are indicated explicitly. We observe that the matrix boundary is closer to the double-trace theory than it is to the quartic matrix model. The stripe critical boundary is, of course, expected to be closer to the $N = 50$ measurement.

(f) *Even model:* This is the model in which we set all odd moments to zero in the action. We get then the double-trace model

$$V = B\mathrm{Tr}M^2 + C\mathrm{Tr}M^4 + D(\mathrm{Tr}M^2)^2. \tag{5.18}$$

The most fundamental property of this model, observed in Monte Carlo simulation, is the absence of the uniform ordered phase. Indeed, only the disorder and the nonuniform order phases exist in the phase diagram. The critical boundary is very close to the double-trace critical line shown in Fig. 7, which consists of two branches. Some precise measurements for

TABLE II. The matrix transition points for $N = 10$–50. These are determined at the point where the eigenvalue distribution splits, which is taken at the value of $\tilde{B}$ where the distribution drops below 0.001 at zero. The search step is 0.025.

$\tilde{C}$	$N = 10$	$N = 25$	$N = 36$	$N = 50$	$\tilde{B}$ extrapolated
2.0	−4.925	−4.475	−4.325	−4.225	−4.090(37)
2.5	−5.225	−4.725	−4.575	−4.475	−4.321(31)
3.0	−5.525	−4.975	−4.875	−4.725	−4.576(36)
4.0	−6.025	−5.525	−5.225	−5.175	−4.993(83)

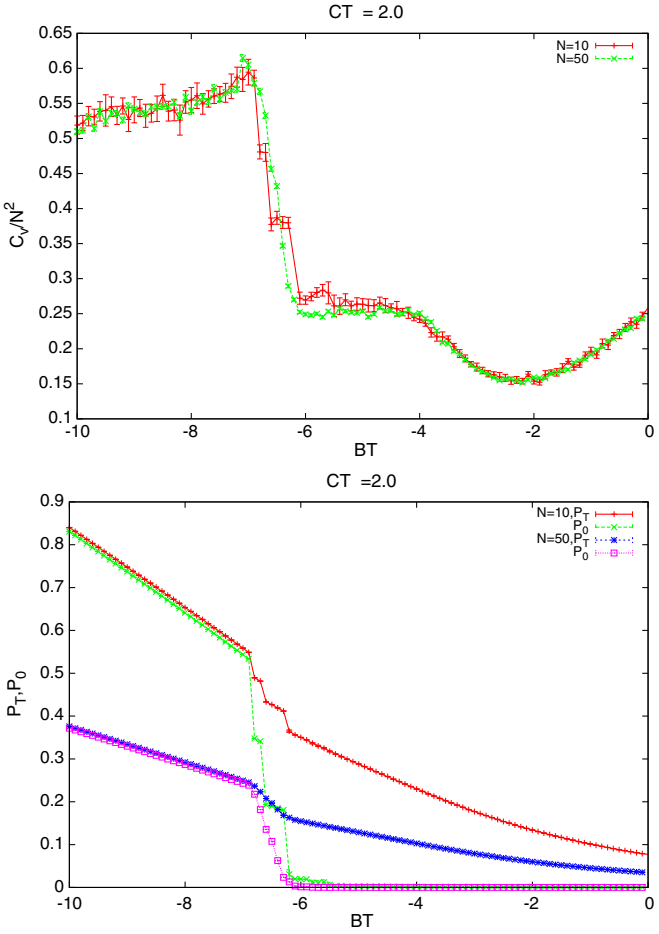

FIG. 5. The total and zero powers and the specific heat, as functions of $\tilde{B}$, of the multitrace model of [18] across the nonuniform-to-uniform transition.

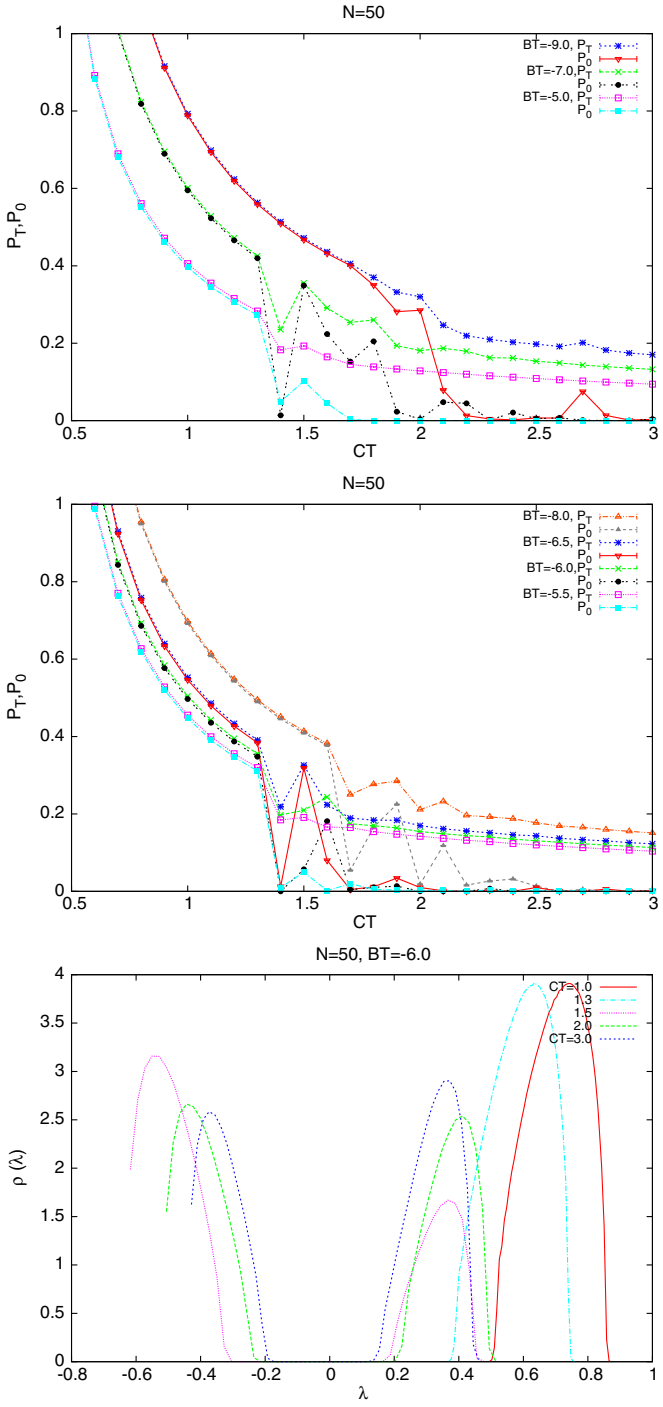

FIG. 6. The total and zero powers, as functions of $\tilde{C}$, and the eigenvalues distribution of the multitrace model of [18] across the nonuniform-to-uniform transition.

the first branch are included in Table IV. The turning point, toward the second branch, occurs around $\tilde{C} \sim 0.1$ where the critical point $-\tilde{B}_*$ becomes increasing, instead of decreasing, as we decrease $\tilde{C}$.

(2) *Model II: Model of* [24]: This model as pointed out previously is the correct approximation of noncommutative scalar Φ_2^4 on the fuzzy sphere. However, this model is characterized by the absence of the uniform ordered phase, and only the matrix transition line separating disordered and nonuniform ordered phases exists in the phase diagram. This fundamental result holds with and without odd terms. The role of the odd terms seems to be negligible, and the two cases with and without odd terms are close. The double-trace theory is also a very good approximation. A phase diagram is attached in Fig. 7.

The second fundamental observation in this case is the existence of a termination point. The matrix critical line does not extend to the origin and terminates at a point around $\tilde{C} = 0.083$ in the case without odd terms, which agrees with the double-trace theory prediction (3.20), and at a point around $\tilde{C} = 0.4$ in the case with odd terms. This termination point is exhibited in Monte Carlo simulation by the failure of the Schwinger-Dyson identity (5.1).

TABLE III. The nonuniform-to-uniform transition points $\tilde{C}$ for $N = 10$–50. These are determined at the discontinuity of the zero power.

$\tilde{B}$	$N = 10$	$N = 25$	$N = 36$	$N = 50$
−9.0	1.95 ± 0.55	1.8 ± 0.4	1.75 ± 0.15	1.95 ± 0.15
−8.0	1.85 ± 0.15	1.65 ± 0.25	1.8 ± 0.2	1.8 ± 0.2
−7.0	1.6 ± 0.4	1.45 ± 0.05	1.55 ± 0.15	1.6 ± 0.3
−6.5	1.65 ± 0.15	1.45 ± 0.05	1.45 ± 0.05	1.45 ± 0.15
−6.0	1.65 ± 0.15	1.35 ± 0.05	1.55 ± 0.05	1.5 ± 0.2
−5.5	1.55 ± 0.05	1.35 ± 0.05	1.35 ± 0.15	1.35 ± 0.05
−5.0	1.45 ± 0.05	1.45 ± 0.05	1.25 ± 0.15	1.4 ± 0.1

In particular, we observe for $N = 50$ that $\tilde{C} = 0.4$ is the smallest value at which the disordered (one-cut) and nonuniform ordered (two-cut) phases are well defined. For $\tilde{C} = 0.2$–0.3 the nonuniform ordered phase cannot be clearly observed, whereas for $\tilde{C} \leq 0.1$ both the disordered and the nonuniform ordered phases become indiscernible. It is therefore natural to identify the triple point with the termination point $\tilde{C} = 0.4$. Our estimation of the termination point is given by

$$(\tilde{B}, \tilde{C}) = (-1.05, 0.4). \tag{5.19}$$

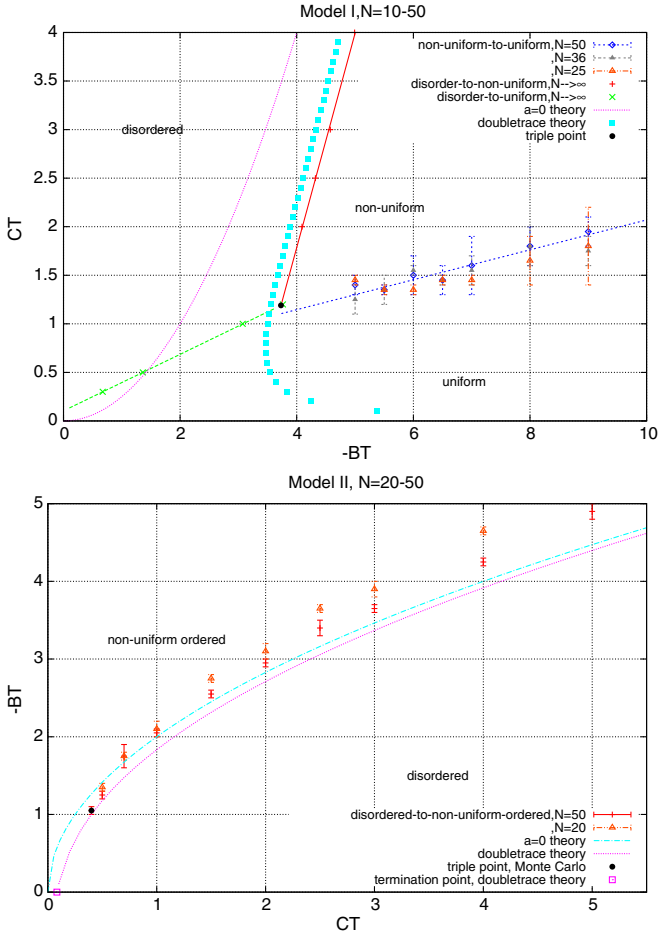

FIG. 7. The phase diagrams of the multitrace models of [18] and [24]. Model I: The Ising and matrix transition data points are not shown but only their extrapolated fits are included, whereas the $N = 25$, $N = 36$, and $N = 50$ stripe data points are indicated explicitly. Model II: The triple point is identified as the termination point located at $(\tilde{B}, \tilde{C}) = (-1.05, 0.4)$ which is to be compared with the double-trace prediction at $(0, 1/12)$.

TABLE IV. The matrix transition points for $N = 10$–50 in Model I without odd terms. In this case only this transition exists and extends to a turning point in accordance with the double-trace theory. The search step is 0.025.

$\tilde{C}$	$N = 10$	$N = 17$	$N = 25$	$N = 36$	$N = 50$	$\tilde{B}$
0.5	−4.325	−4.225	−4.025	−3.875	−3.825	−3.738(72)
1	−4.375	−4.175	−4.025	−3.875	−3.775	−3.685(54)
2	−4.925	−4.675	−4.475	−4.325	−4.225	−4.098(50)
3	−5.475	−5.275	−5.025	−4.825	−4.725	−4.601(84)
5	−6.525	−6.275	−6.025	−5.725	−5.625	−5.479(108)

D. Grosse-Wulkenhaar model

The multitrace approach can also be applied to a regularized noncommutative Φ_2^4 on the Moyal-Weyl plane in the matrix basis [24] with action given by

$$S = \mathrm{Tr}_N \left[\frac{1}{2} m^2 M^2 + \frac{u}{N} M^4 + a(EM^2 + \sqrt{\omega}\Gamma^+ M \Gamma M) \right]. \tag{5.20}$$

Two cases are of importance to us here:

(1) The noncommutative theory without a harmonic oscillator term. In this case the effective action takes the form

$$\begin{aligned} S_{\text{effe}} &= b\mathrm{Tr}_N M^2 + c\mathrm{Tr}_N M^4 + d(\mathrm{Tr}_N M^2)^2 \\ &\quad + b_1(\mathrm{Tr}_N M)^2 + c_1(\mathrm{Tr}_N M)^4 \\ &\quad + d_1 \mathrm{Tr}_N M^2 (\mathrm{Tr}_N M)^2 + e\mathrm{Tr}_N M \mathrm{Tr}_N M^3. \end{aligned} \tag{5.21}$$

The parameters are given by

$$\begin{aligned} &b = \frac{m^2}{2} + \frac{aN}{2}, \quad c = \frac{u}{N} - \frac{a^2 N}{24}, \quad d = -\frac{a^2}{12} \\ &b_1 = -\frac{a}{2}, \quad c_1 = \frac{a^2}{24N^2}, \quad d_1 = -\frac{a^2}{12N}, \quad e = \frac{a^2}{6}. \end{aligned} \tag{5.22}$$

If we assume the symmetry $M \to -M$, then all odd moments vanish identically and we end up with the action

$$S_{\text{effe}} = b\text{Tr}_N M^2 + c\text{Tr}_N M^4 + d(\text{Tr}_N M^2)^2. \quad (5.23)$$

(2) At the self-dual point we have $\Omega^2 = 1$, and thus $\sqrt{\omega} = 0$, and as a consequence the effective action reduces to the multitrace model

$$S_{\text{effe}} = b\text{Tr}_N M^2 + c\text{Tr}_N M^4 + d(\text{Tr}_N M^2)^2. \quad (5.24)$$

The parameters b, c, and d are given by

$$b = \frac{m^2}{2} + \frac{aN}{2}, \qquad c = \frac{u}{N} - \frac{a^2 N}{24}, \qquad d = \frac{a^2}{24}. \quad (5.25)$$

Both the actions (5.23) and (5.24) do not contain odd moments, and thus the corresponding phase diagrams are expected to not contain the uniform ordered phase with all matrixlike behavior as a consequence.

VI. CONCLUSION

A Monte Carlo study of the multitrace quartic matrix model of [18], which is claimed to be the first nontrivial correction to noncommutative Φ^4 on the fuzzy sphere, is presented. This model does not suffer from the severe ergodic problems encountered in the simulations of noncommutative Φ^4 on the fuzzy sphere, and the Metropolis algorithm is very effective in probing the entire phase space. In particular, Monte Carlo measurement of the one-cut-to-two-cut and the Ising transition lines as well as a direct Monte Carlo measurement of the nonuniform-to-uniform transition line are performed. The odd terms in the action that are dropped in [18] do play the central role in generating the Ising phase and the nonuniform-to-uniform transition line and thus a triple point. A quantitative sketch of the phase diagram and the triple point is outlined.

The closely related multitrace quartic matrix model of [24], which is the correct approximation of noncommutative scalar Φ_2^4 on the fuzzy sphere, is also considered in this article where it is shown that the one-cut-to-two-cut transition line does not extend to the origin and terminates at a point consistent with the triple point of noncommutative Φ^4 on the fuzzy sphere [11].

We also commented in this article on the Grosse-Wulkenhaar model, which is examined using a combination of the multitrace technique and the Monte Carlo method. At this order of the multitrace approximation the two models obtained in this case do not exhibit the Ising phase and the nonuniform-to-uniform transition line.

ACKNOWLEDGMENTS

This research was supported by CNEPRU: "The National (Algerian) Commission for the Evaluation of University Research Projects" under Contract No. DO 11 20 13 00 09.

APPENDIX: SUSCEPTIBILITY AND SPECIFIC HEAT

1. Susceptibility

We consider Φ^4 on the fuzzy sphere coupled to a constant magnetic field H given by the action

$$S = \text{Tr}(a\Phi[L_a, [L_a, \Phi]] + b\Phi^2 + c\Phi^4 + H\Phi). \quad (A1)$$

The magnetization and the susceptibility are defined by

$$\text{magnetization} = \frac{1}{N}\langle \text{Tr}\Phi \rangle = -\frac{1}{N}\frac{\partial}{\partial H}\ln Z, \quad (A2)$$

$$\text{susceptibility} = \langle (\text{Tr}\Phi)^2 \rangle - \langle \text{Tr}\Phi \rangle^2 = \frac{\partial^2}{\partial H^2}\ln Z = -N\frac{\partial}{\partial H}\text{magnetization}. \quad (A3)$$

On the fuzzy sphere we have

$$x_a = \frac{2R}{N}L_a, \qquad [x_a, x_b] = \frac{i\theta}{R}\epsilon_{abc}x_c, \qquad \theta = \frac{2R^2}{N}, \qquad \text{Tr} = \frac{N}{4\pi R^2}\int d^2x. \quad (A4)$$

The regularized noncommutative plane is then defined by

$$x_3 = R, \qquad [x_1, x_2] = i\theta, \qquad \partial_i = -\frac{1}{R}\epsilon_{ij}L_j = -\frac{1}{\theta}\epsilon_{ij}x_j, \qquad \int d^2x = 2\pi\theta\text{Tr}. \quad (A5)$$

We have $\epsilon_{12} = 1$. The above action becomes, including a rescaling of the field $\Phi \to \phi = \sqrt{Na/2\pi}\Phi$, given by the equation

$$S = 2\pi\theta\text{Tr}\left(\frac{1}{2}\phi\partial_i\partial_i\phi + \frac{1}{2}m^2\phi^2 + \frac{1}{4}\lambda\phi^4 + h\phi\right), \quad (A6)$$

$$m^2 = \frac{b}{aR^2}, \qquad \lambda = \frac{4\pi c}{Na^2R^2}, \qquad h = \sqrt{\frac{N}{2\pi a}}\frac{H}{2R^2}. \quad (A7)$$

The commutative limit is $\theta \to 0$. By using a lattice in this limit we have

$$S = l^2 \sum_n \left(\frac{1}{2} (\phi \partial_i \partial_i \phi)_{\text{lattice}} + \frac{1}{2} m^2 \phi_n^2 + \frac{1}{4} \lambda \phi_n^4 + h \phi_n \right). \tag{A8}$$

We compute in this limit on the lattice

$$\begin{aligned} \text{magnetization} &= \frac{1}{N} \langle \text{Tr}\Phi \rangle \\ &\to \frac{\mathcal{N}^2 l^2}{4\pi R^2} \left\langle \frac{1}{\mathcal{N}^2} \sum_n \Phi_n \right\rangle. \end{aligned} \tag{A9}$$

The volume of the lattice must be equal to the area of the sphere, viz. $\mathcal{N}^2 l^2 = 4\pi R^2$. Also we compute

$$\begin{aligned} \text{susceptibility} &= \langle (\text{Tr}\Phi)^2 \rangle - \langle \text{Tr}\Phi \rangle^2 \\ &= \frac{N^2}{\mathcal{N}^4} \frac{\mathcal{N}^2 l^2}{4\pi R^2} \left(\left\langle \left(\sum_n \Phi_n \right)^2 \right\rangle - \left\langle \sum_n \Phi_n \right\rangle^2 \right). \end{aligned} \tag{A10}$$

2. Specific heat

The specific heat is defined by

$$\begin{aligned} C_v &= \frac{\partial^2}{\partial \beta^2} \ln Z \\ &= \langle S^2 \rangle - \langle S \rangle^2. \end{aligned} \tag{A11}$$

The inverse temperature is introduced in the usual way as

$$Z = \int dM \exp(-\beta S[M]). \tag{A12}$$

The calculation of the effective potential proceeds as before with the replacement $a \to a\beta$. The partition function in the quartic multitrace approximation is

$$\begin{aligned} Z = & \int d\Lambda \Delta^2(\Lambda) \exp(-\beta V_0) \\ & + \beta \int d\Lambda \Delta^2(\Lambda) \exp(-\beta V_0)(-V_2) \\ & + \beta^2 \int d\Lambda \Delta^2(\Lambda) \exp(-\beta V_0) \left(-V_4 + \frac{1}{2} V_2^2 \right). \end{aligned} \tag{A13}$$

A straightforward calculation yields

$$C_v = \langle (V + V_4)^2 \rangle - \langle (V + V_4) \rangle^2 - 2 \langle V_4 + 2V_4^2 + 2V_2 V_4) \rangle. \tag{A14}$$

The last term could make this approximation of the specific heat negative. This actually happens in the approximation of [18].

[1] S. A. Brazovkii, Phase transition of an isotropic system to a nonuniform state, Zh. Eksp. Teor. Fiz. **68**, 175 (1975).

[2] S. Minwalla, M. Van Raamsdonk, and N. Seiberg, Noncommutative perturbative dynamics, J. High Energy Phys. 02 (2000) 020.

[3] S. S. Gubser and S. L. Sondhi, Phase structure of noncommutative scalar field theories, Nucl. Phys. **B605**, 395 (2001).

[4] J. Ambjorn, Y. M. Makeenko, J. Nishimura, and R. J. Szabo, Lattice gauge fields and discrete noncommutative Yang-Mills theory, J. High Energy Phys. 05 (2000) 023.

[5] J. Ambjorn and S. Catterall, Stripes from (noncommutative) stars, Phys. Lett. B **549**, 253 (2002).

[6] H. Grosse and R. Wulkenhaar, Renormalisation of ϕ^4 theory on noncommutative R^2 in the matrix base, J. High Energy Phys. 12 (2003) 019.

[7] J. Hoppe, Quantum theory of a massless relativistic surface and a two-dimensional bound state problem, Ph.D thesis, MIT, 1982.

[8] J. Madore, The fuzzy sphere, Classical Quantum Gravity **9**, 69 (1992).

[9] A. Connes, *Noncommutative Geometry* (Academic Press, London, 1994).

[10] J. Frohlich and K. Gawedzki, Conformal field theory and geometry of strings, in *Proceedings of Mathematical Quantum Theory Conference Vancouver, British Columbia, Canada* (1993).

[11] F. Garcia Flores, X. Martin, and D. O'Connor, Simulation of a scalar field on a fuzzy sphere, Int. J. Mod. Phys. A **24**, 3917 (2009).

[12] F. Garcia Flores, D. O'Connor, and X. Martin, Simulating the scalar field on the fuzzy sphere, *Proc. Sci.*, LAT20052006 (2006) 262.

[13] X. Martin, A matrix phase for the ϕ^4 scalar field on the fuzzy sphere, J. High Energy Phys. 04 (2004) 077.

[14] M. Panero, Numerical simulations of a non-commutative theory: The scalar model on the fuzzy sphere, J. High Energy Phys. 05 (2007) 082.

[15] J. Medina, W. Bietenholz, and D. O'Connor, Probing the fuzzy sphere regularisation in simulations of the 3d $\lambda\phi^4$ model, J. High Energy Phys. 04 (2008) 041.

[16] C. R. Das, S. Digal, and T. R. Govindarajan, Finite temperature phase transition of a single scalar field on a fuzzy sphere, Mod. Phys. Lett. A **23**, 1781 (2008).
[17] B. Ydri, New algorithm and phase diagram of noncommutative ϕ^4 on the fuzzy sphere, J. High Energy Phys. 03 (2014) 065.
[18] D. O'Connor and C. Saemann, Fuzzy scalar field theory as a multitrace matrix model, J. High Energy Phys. 08 (2007) 066.
[19] C. Saemann, The multitrace matrix model of scalar field theory on fuzzy CP^n, SIGMA **6**, 050 (2010).
[20] A. P. Polychronakos, Effective action and phase transitions of scalar field on the fuzzy sphere, Phys. Rev. D **88**, 065010 (2013).
[21] J. Tekel, Uniform order phase and phase diagram of scalar field theory on fuzzy CP^n, J. High Energy Phys. 10 (2014) 144.
[22] V. P. Nair, A. P. Polychronakos, and J. Tekel, Fuzzy spaces and new random matrix ensembles, Phys. Rev. D **85**, 045021 (2012).
[23] J. Tekel, Random matrix approach to scalar fields on fuzzy spaces, Phys. Rev. D **87**, 085015 (2013).
[24] B. Ydri, A multitrace approach to noncommutative Φ_2^4, arXiv:1410.4881 [Phys. Rev. D (to be published)].
[25] H. Steinacker, A non-perturbative approach to non-commutative scalar field theory, J. High Energy Phys. 03 (2005) 075.
[26] W. Bietenholz, F. Hofheinz, and J. Nishimura, Phase diagram and dispersion relation of the noncommutative $\lambda\Phi^4$ model in $d = 3$, J. High Energy Phys. 06 (2004) 042.
[27] F. Lizzi and B. Spisso, Noncommutative field theory: Numerical analysis with the fuzzy disc, Int. J. Mod. Phys. A **27**, 1250137 (2012).
[28] H. Meja-Daz, W. Bietenholz, and M. Panero, The continuum phase diagram of the 2d non-commutative $\lambda\Phi^4$model, J. High Energy Phys. 10 (2014) 56.
[29] U. Wolff, Collective Monte Carlo Updating for Spin Systems, Phys. Rev. Lett. **62**, 361 (1989).
[30] L. Onsager, Crystal statistics. 1. A two-dimensional model with an order disorder transition, Phys. Rev. **65**, 117 (1944).
[31] Y. Shimamune, On the phase structure of large N matrix models and gauge models, Phys. Lett. B **108**, 407 (1982).
[32] B. Eynard, Random Matrices, Cours de Physique Theorique de Saclay.
[33] E. Brezin, C. Itzykson, G. Parisi, and J. B. Zuber, Planar diagrams, Commun. Math. Phys. **59**, 35 (1978).
[34] N. Kawahara, J. Nishimura, and A. Yamaguchi, Monte Carlo approach to nonperturbative strings—Demonstration in noncritical string theory, J. High Energy Phys. 06 (2007) 076.